Bull. Inst. Chem. Res., Kyoto Univ., Vol. 60, No. 2, 1982

Inelastic Scattering of 28.5 MeV Alpha Particles by ^{60}Ni and ^{62}Ni

Isao KUMABE*, Masaru MATOBA**, Makoto INOUE***,
Seishi MATSUKI**** and Eiichi TAKASAKI*****

Received March 12, 1982

The angular distributions of alpha particles elastically and inelastically scattered by ^{60}Ni and ^{62}Ni have been measured at 28.5 MeV. About 40 angular distributions, which include those corresponding to the so-called two-phonon triplet, have been obtained. Results were analyzed in terms of the optical model and the DWBA theory. The observed cross sections for excitation of the two-phonon triplet states were compared with the predictions of the coupled channel theory, and a reasonable agreement between the experiment and the theory has been obtained. Inelastic scatterings leading to the first 2^+, the first 4^+ and the first 0^+ states of ^{62}Ni were analyzed using form factors of a microscopic model. The so-called two-phonon states, some possible 3^- states other than the most prominent ones and possible higher spin (5^-) states are discussed.

KEY WORDS: NUCLEAR REACTION ^{60,62}Ni(α, α') E=28.5 Mev; measured $\sigma(E_{\alpha'}, \theta)$/ ^{60,62}Ni deduced levels/ J, π, deformation parameters/ Enriched targets/

I. INTRODUCTION

The study of the inelastic scattering of medium energy particles has proved to be a powerful tool for determining the spin and parity as well as the detailed information on the wave function of the nuclear excited states. Especially, inelastic scattering of alpha particles by nuclei is known to excite strongly the states of collective character.

The first-order DWBA theory[1] has accurately explained both the angular distributions and magnitudes of cross sections for inelastic scattering leading to one-phonon states. This fact makes it possible to determine spin-parities of nuclear states.

However, the first-order DWBA theory is not adequate for describing transitions to so-called two-phonon states of nuclei. Buck[2] and Tamura[3] have successfully explained the second-order process using the coupled-channel equations. As the theory attempts to account for detailed properties of nuclei, accurate experimental data are desirable.

Many experimental studies of inelastic alpha scattering have been performed for medium weight nuclei. Several workers[4] have reported about the excitation of two-

* 隈部 功: Department of Nuclear Engineering, Kyushu University, Fukuoka.
** 的場 優: Department of Energy Conversion Engineering, Graduate School of Engineering Sciences, Kyushu University, Fukuoka.
*** 井上 信: Research Center for Nuclear Physics, Osaka University, Suita, Osaka.
**** 松木征史: Laboratvry of Nuclear Reaction, Institute for Chemical Research, Kyoto University, Kyoto.
***** 高崎栄一: National Laboratory for High Energy Physics, Oho-machi, Tsukuba-gun, Ibaraki.

phonon states by inelastic alpha scattering. However, most of them have reported a two phonon 4^+ state and have not completely resolved the two-phonon triplet states. Experiments in which tho two-phonon triplet states are completely resolved are desirable for understanding the properties of these states.

Some of the authors and others[5,6] have measured the angular distributions of alpha particles for all of the two-phonon triplet states of ^{60}Ni at 34.4 MeV. This result has been analysed by Tamura[7] with the coupled-channel method and have been successfully explained as an interference effect between two possible modes for exciting the two-phonon states, *i. e.*, a direct transition and a multiple transition. Therefore, it is interesting to see how well the coupled-channel method predicts the angular distributions for the two-phonon triplet states measured at different bombarding energies and/or with different target-nuclei. Thus the present experiment was undertaken to investigate the angular distributions for the two-phonon triplet states of ^{60}Ni and ^{62}Ni at 28.5 MeV under the condition of good energy resolution.

Nickel isotopes are single closed shell nuclei and are suitable for detailed comparison with the microscopic description of inelastic scattering[8], where appropriate such analyses were carried out.

Octupole states other than the prominent one have been observed in some experimemts. Veje[9] has calculated excitation energies and reduced transition probabilities of octupole vibrational states with the microscopic theory on the basis of an interaction consisting of pairing plus octupole-octupole force. The distribution of isoscalar octupole strength in many medium weight nuclei have been studied using (α, α') experiments[10,11] and a prominent broad peak ($\Gamma \sim 2.5$ MeV) was observed[10] at $E_x \sim 30A^{-1/3}$ MeV. However no broad peak was observed in this excitation energy range in ^{208}Pb or ^{40}Ca and lighter nuclei. The angular distributions of the (α, α') reaction exciting these peaks were in excellent agreement with $l=3$ DWBA calculations. This low-energy octupole resonance (LEOR) was found[10] to exhaust 20~30% of the isoscalar E3 strength allowed by the energy weighted sum rule (EWSR).

It should be noted that no LEOR is found for ^{58}Ni and only three discrete states between 6 and 7.9 MeV which exhaust only ~10% of the E3 strength allowed by EWSR were observed[6,10] for ^{58}Ni. In this situation it is interesting to investigate octupole states other than the prominent one in Ni isotopes because one has a question whether this fact is general in this mass region or not. Thus the another purpose of the present experiment is to investigate possible 3^- states and to compare them with the theory.

The experimental angular distributions covered a wide angular range (15°~110°) to investigate the behaviour of the optical-model parameters and to obtain more detailed informations concerning the inelastic scattering.

II. EXPERIMENTAL PROCEDURE

Experimental procedures were similar to those of the previous work.[12]

A beam of alpha particles from the 105 cm Kyoto University cyclotron was analysed by a beam analysing magnet and brought into a scattering chamber. The average

alpha-particle energy in the target foils was estimated to be 28.5 MeV.

Nickel 60 and nickel 62 targets were self-supporting metallic foils. Each target was prepared by electroplating onto a thin copper foil and then dissolving the copper foil with activated acid.[13] The targets consisted of isotopically enriched ^{60}Ni and ^{62}Ni whose thicknesses were 0.76 and 0.72 mg/cm^2, respectively.

The targets were placed at 60° with respect to the bombarding beam in order to minimize the energy spread due to the energy loss of alpha parricles in the targets for scattering angles; 20°-60° and Q values; 0—-5 MeV.

Scattered alpha particles were detected simultaneously by two 0.5 mm thick silicon surface barrier detectors. Alpha particles scattered at forward angles from 15° to 60° were detected by a forward detector, while those scattered at backward angles from 60° to 105° were detected simultaneously by a backward detector. A defining aperture of 1 mm wide and 4 mm high was placed just in front of the forward detector and was situated 95.4 mm from the target. A defining aperture of 1 mm wide and 5 mm high was placed just in front of the backward detector and was situated 57.6 mm from the target. In order to reject electrons emitted from the target, a small permanent magnet was set in front of each defining aperture.

The beam direction was determined by taking data on each side of the beam. Because of the rapid variation with angle of the scattering cross sections, the direction could be measured with an accuracy less than 0.2°.

The over-all energy resolution (full width at half maximum) was about 70 keV which includes a beam energy spread of 45 keV, amplifier and detector noises of about 30 keV, a target effect of about 30 keV and a kinematical energy spread of about 30 keV.

The energies of scattered particles were calibrated using the positions of elastic peak and inelastic peaks corresponding to the first 2^+ state and the prominent 3^- state, whose energies were well known. For ^{60}Ni most of the energy values were taken from Ref. 6.

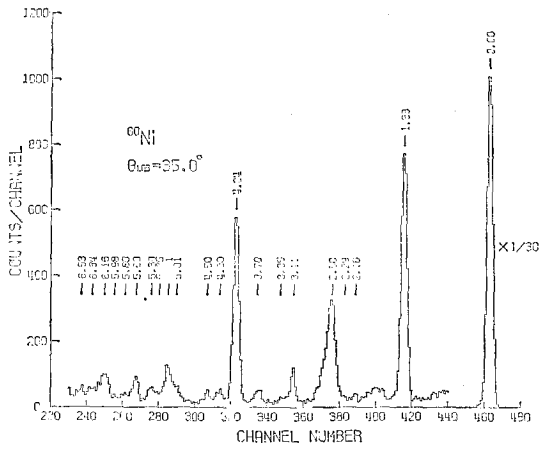

Fig. 1. Typical energy spectrum of alpha particles scattered by ^{60}Ni at a laboratory angle of 35.0°. The energy levels corresponding to the peaks are shown in the upper part of the figure.

III. EXPERIMENTAL RESULTS

Typical pulse height spectra of the alpha paricles scattered by ^{60}Ni and ^{62}Ni are shown in Figs. 1 and 2, respectively.

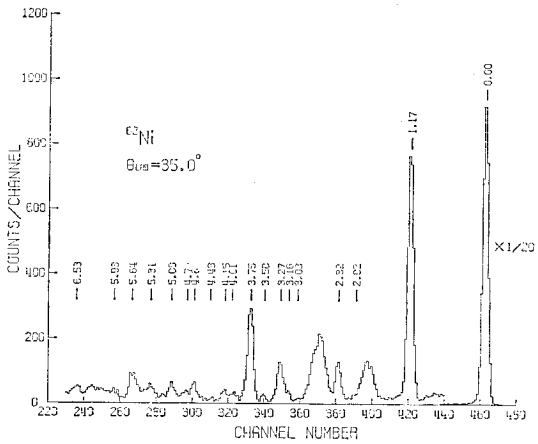

Fig. 2. Typical energy spectrum of alpha particles scattered by ^{62}Ni at a laboratory angle 35.0°. The energy levels corresponding to the peaks are shown in the upper part of the figure.

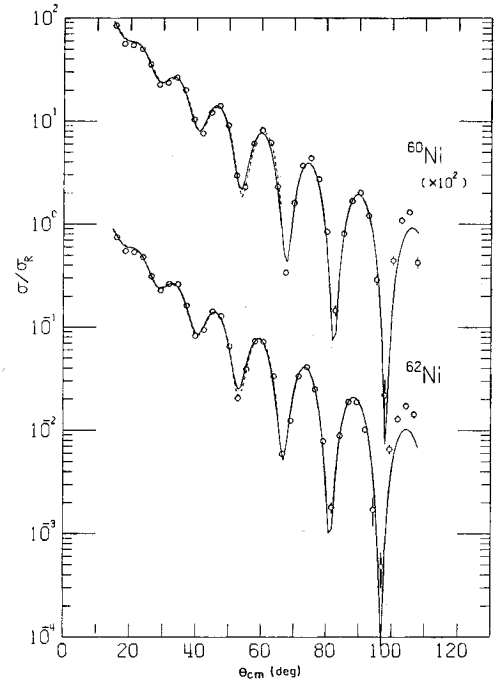

Fig. 3. Measured elastic scattering from ^{60}Ni and ^{62}Ni and the optical model fits. The dashed curves are the predictions of the potentials 1 and 4 and the solid curves are those of the potentials 7 and 10.

The angular distributions for elastic scattering are shown in Fig. 3 and those for inelastic scattering are shown in Figs. 4 and 5.

The angular distributions for the first 2^+ state and the prominent 3^- state are out of phase and in phase, respectively, with the elastic angular distribution and are in agreement with the Blair phase rule.[14]

On the other hand, the oscillation in the angular distribution for the presumed second 2^+ state is almost out of phase with that predicted for single excitation of a 2^+ level, while those for the 4^+ states are in almost accord with the predictions for single excitation of this multipolarity. The angular distribution for weakly excited 0^+ state of ^{60}Ni fits reasonably well the predictions for single excitation but shows some indication of slipping out of phase with the single-excitation predictions at larger angles, while that for weakly excited 0^+ state of ^{62}Ni shows some indication of slipping out of phase with the single-excitation predictions at all angles.

Several angular distributions, which were in phase with the prominent 3^- inelastic

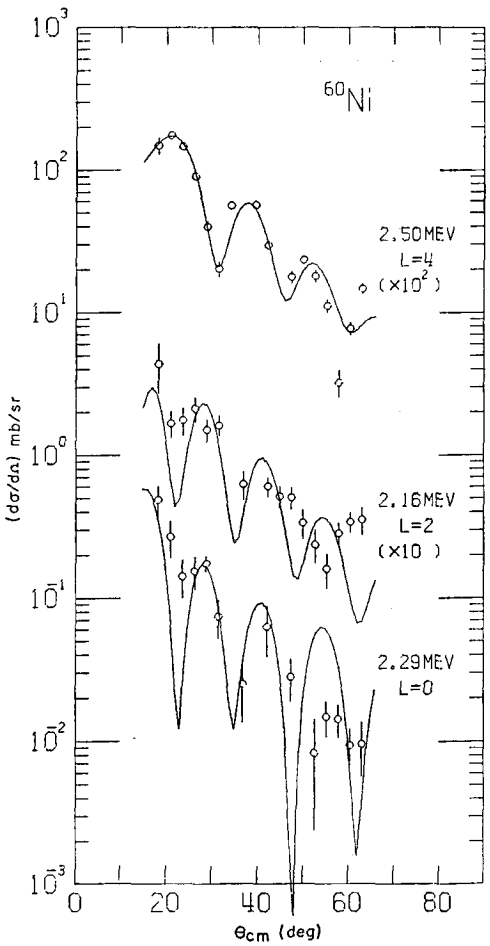

Fig. 4-a

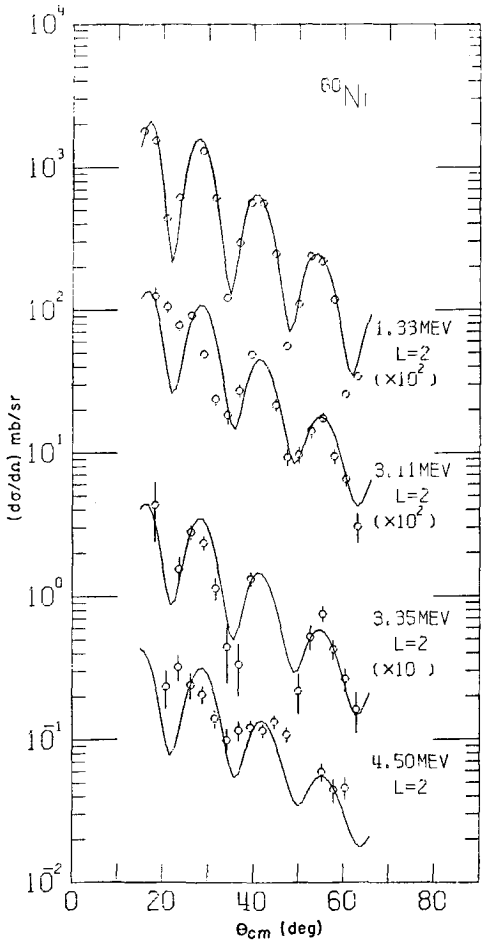

Fig. 4-b

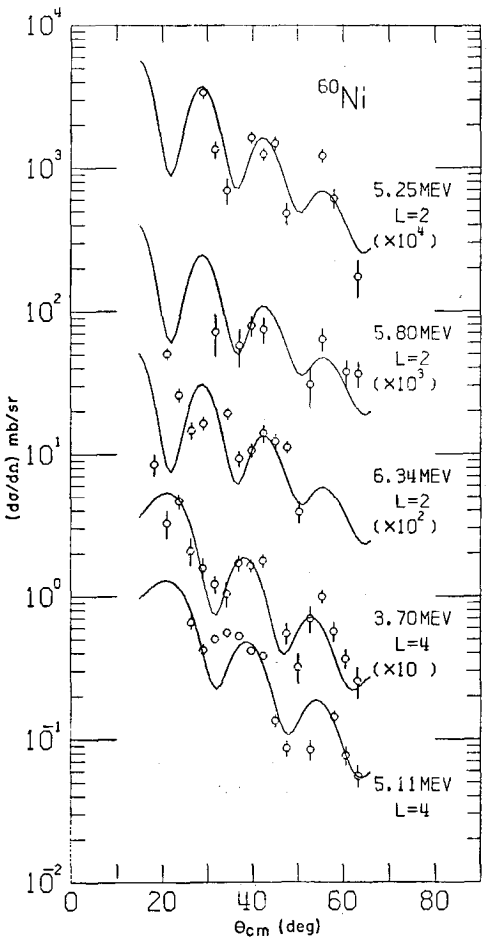
60Ni
5.25MEV
L=2
(×10⁴)
5.80MEV
L=2
(×10³)
6.34MEV
L=2
(×10²)
3.70MEV
L=4
(×10)
5.11MEV
L=4
(dσ/dΩ) mb/sr
θcm (deg)

Fig. 4-c

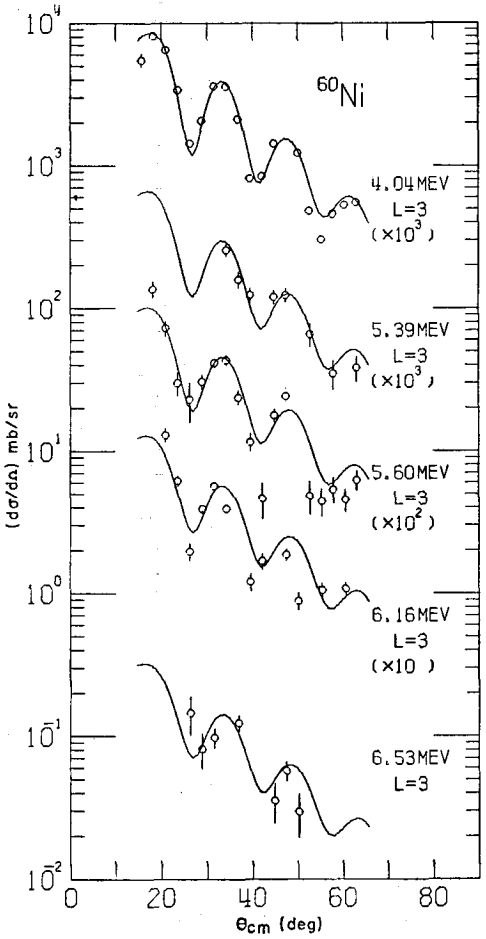
60Ni
4.04MEV
L=3
(×10³)
5.39MEV
L=3
(×10³)
5.60MEV
L=3
(×10²)
6.16MEV
L=3
(×10)
6.53MEV
L=3
(dσ/dΩ) mb/sr
θcm (deg)

Fig. 4-d

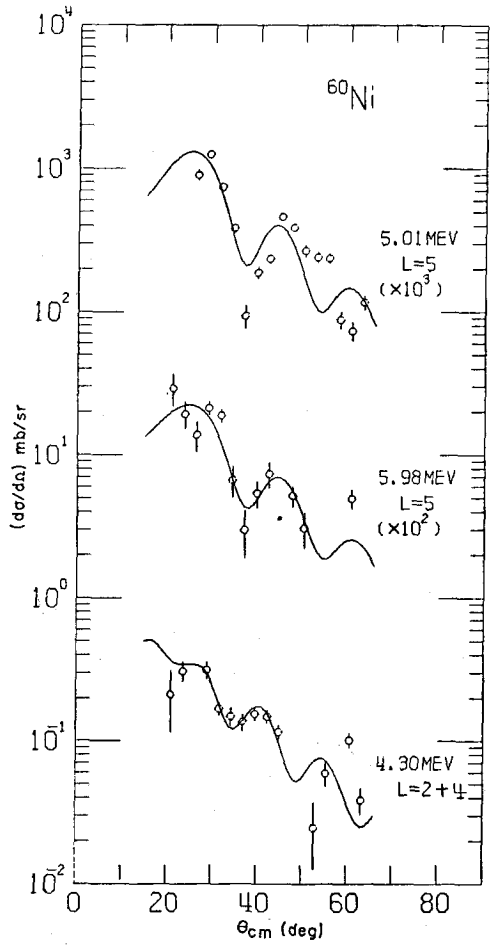

Fig. 4-e

Fig. 4. Measured angular distributions for Inelastic scattering leading to the various states of ^{60}Ni. The solid curves are the DWBA predictions.

distribution were obtained. These are the 5.39, 5.60, 6.16 and 6.53 MeV peaks of ^{60}Ni and the 4.43, 4.65, 5.64 and 6.53 MeV peaks of ^{62}Ni.

The angular distributions for the states whose angular momenta may be assigned to be five were also obtained. They are the 5.01 and 5.98 MeV peaks of ^{60}Ni and the 4.15 MeV peak of ^{62}Ni.

The angular distributions covering a wide angular range were obtained for the strongly excited states and shown in Fig. 6.

The 2.32 MeV peak of ^{62}Ni is an unresolved group of the two-phonon 2^+ and 4^+ states. As is seen in Fig. 4(a), the cross section of the 4^+ state is about ten times as large as that of the 2^+ state. Therefore in the following analyses this peak was assumed to correspond to the 4^+ state only.

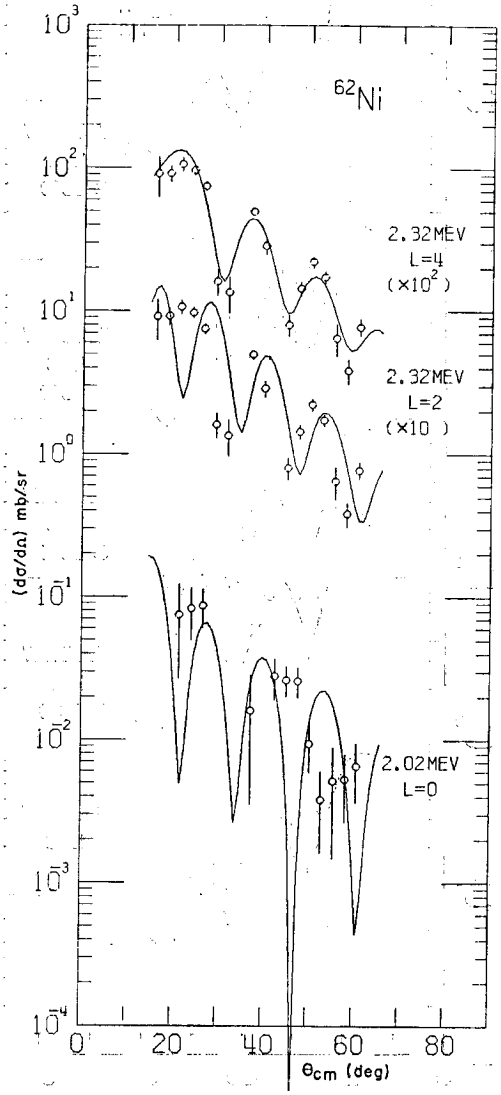
^{62}Ni
2.32MEV
L=4
(×10^2)
2.32MEV
L=2
(×10)
2.02MEV
L=0
(dσ/dΩ) mb/sr
θcm (deg)

Fig. 5-a

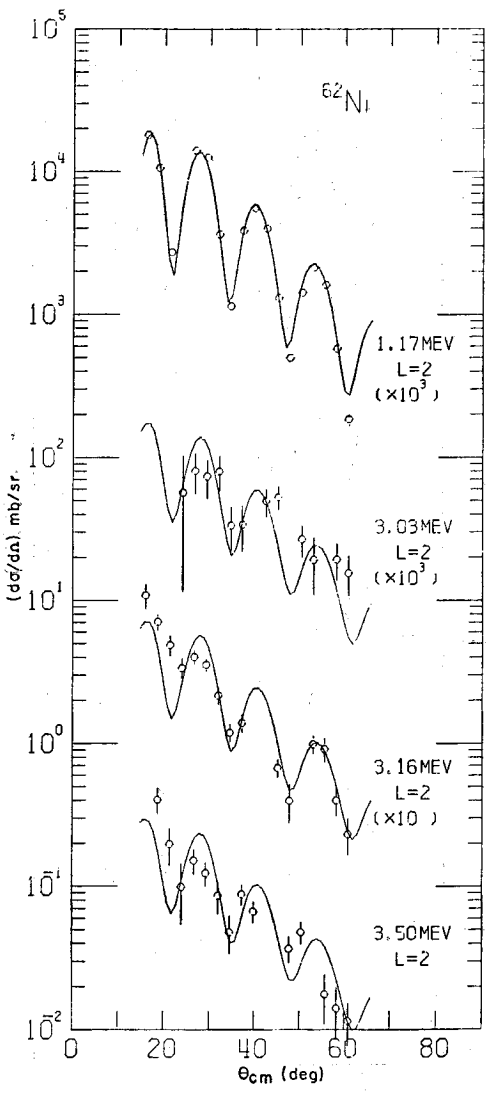
^{62}Ni
1.17MEV
L=2
(×10^3)
3.03MEV
L=2
(×10^3)
3.16MEV
L=2
(×10)
3.50MEV
L=2
(dσ/dΩ) mb/sr
θcm (deg)

Fig. 5-b

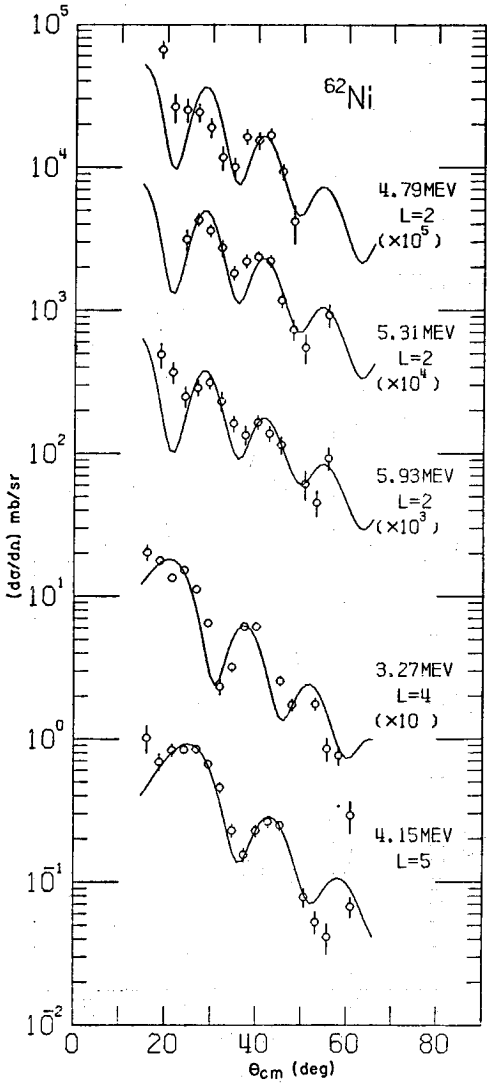

Fig. 5-c

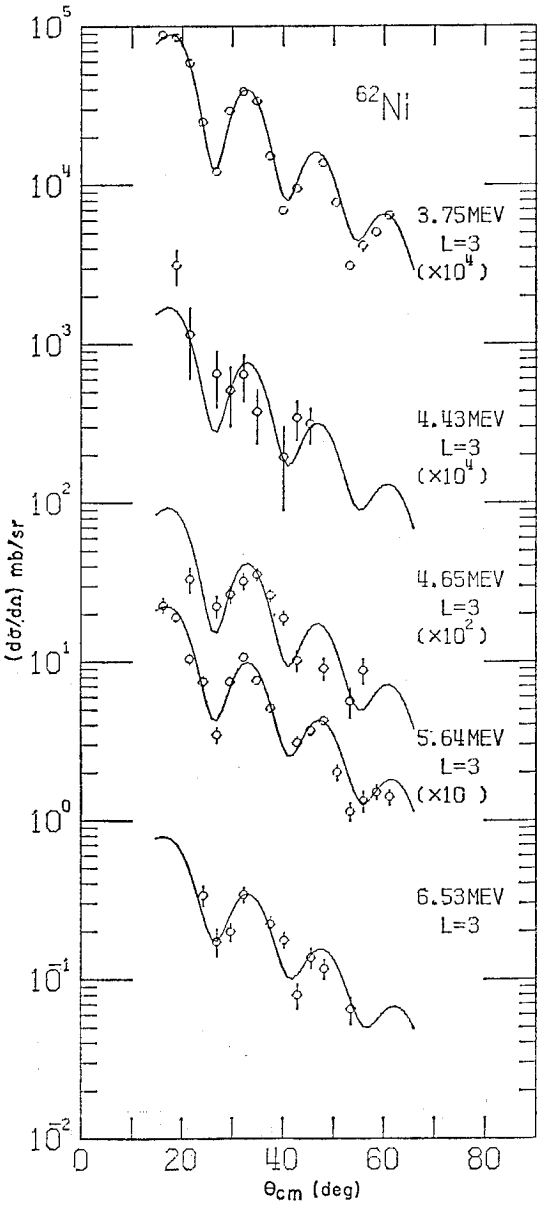

Fig. 5-d

Fig. 5. Measured angular distributions for inelastic scattering leading to the various states of ^{62}Ni. The solid curves are the DWBA predictions.

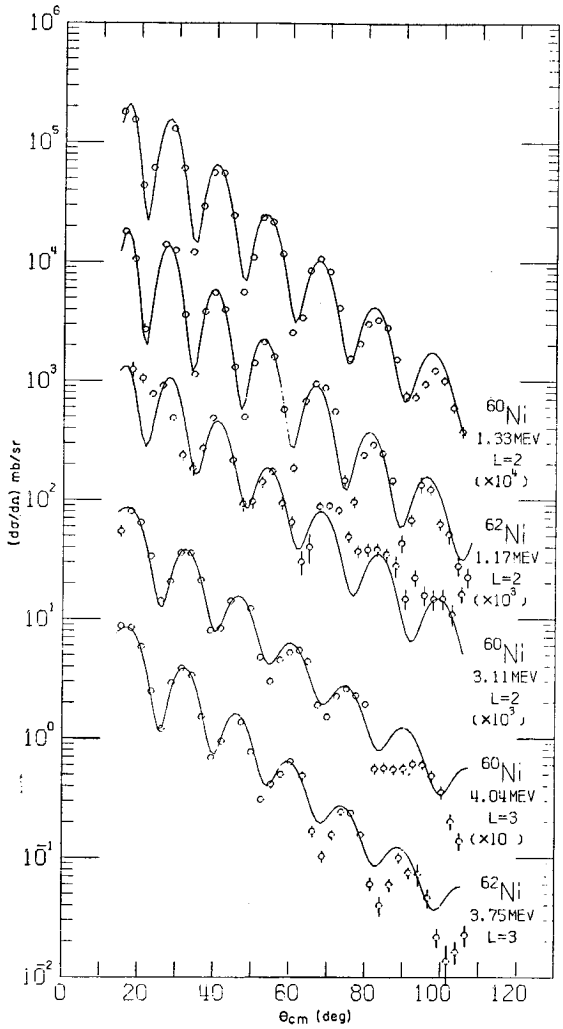

Fig. 6. The angular distributions covering a wide angular range obtained for the strongly excited states of ^{60}Ni and ^{62}Ni. The solid curves are the DWBA predictions.

IV. DATA ANALYSES

IV. 1. The optical model

For the elastic angular distributions, an optical-model analysis was performed. The optical potential used has the form

$$U(r) = -(V+iW)(e^x+1)^{-1}$$
$$x = (r - r_0 A^{1/3})/a,$$

to which is added the Coulomb potential from a uniformly charged sphere of radius $r_c A^{1/3}$.

Table I Optical potentials for 28.5 MeV alpha particles on ^{60}Ni and ^{62}Ni

		V (MeV)	W (MeV)	r_0 (MeV)	a (fm)	r_c (fm)	χ^2/n
$\theta<65°$							
^{60}Ni	1	50.281	11.320	1.5728	0.5631	1.3	1.13
	2	103.603	15.191	1.4879	0.5543	1.3	1.32
	3	214.668	21.705	1.3946	0.5472	1.3	1.48
^{62}Ni	4	48.107	11.666	1.5894	0.5600	1.3	0.776
	5	99.361	15.244	1.5023	0.5490	1.3	0.921
	6	205.373	21.546	1.4112	0.5417	1.3	1.09
all θ							
^{60}Ni	7	48.701	12.077	1.5985	0.5606	1.3	7.35
	8	109.753	18.316	1.4772	0.5614	1.3	12.3
	9	231.442	28.822	1.3701	0.5608	1.3	15.0
^{62}Ni	10	49.102	12.469	1.5915	0.5557	1.3	6.31
	11	109.757	18.869	1.4749	0.5570	1.3	11.3
	12	237.172	29.947	1.3610	0.5605	1.3	13.2

The first set of potentials optimizes the fit to the data for $\theta<65°$ only, the second set was fitted to all the data.

Fits to the data were obtained by varying the parameters of the potential so as to minimize the mean square deviation between the experimental and predicted cross sections. The minimization was performed using an automatic search routine.[15]

In the present analysis the quantity χ^2/point was calculated assuming the relative cross-section errors of 5%. As is well known,[16] alpha-particle scattering does not yield a unique potential. Therefore, in Table I three sets of potential parameters of depth V of about 50, 120 and 200 MeV are given for each isotope. Table I lists also two sets of potential parameters which optimize the fit to the data for $\theta<65°$ only and to all the data.

The angular distributions predicted by the potentials 1, 4, 7 and 10 are compared with the experimental angular distributions in Fig. 3, where the ratio of cross section to the Rutherford scattering is presented. The dashed curves are the predictions of the potentials 1 and 4, and the solid curves are those of the potentials 7 and 10. The potentials 2, 3, 5, 6, 8, 9, 11 and 12 reproduced nearly the same angular distributions as those predicted by the potentials 1, 4, 7 and 10, respectively.

The potentials 1 and 4 were used for the following DWBA calculation except for the angular distributions covering a wide angular range. For the angular distributions shown in Fig. 6 the potentials 7 and 10 were used.

IV. 2. DWBA Analysis

The DWBA analysis with the macroscopic form factor, which is the derivative of the Woods-Saxon potential, was applied to all the inelastic angular distributions using the INS-DWBA 2 code.[17] The calculated angular distributions using the first derivative Saxon form factors are shown in Figs. 4~6. Except for some of the so-called two-phonon

states, the agreement between theory and experiment is sufficiently good to enable us to make spin-parity assignments. All the curves include Coulomb excitation.

Martens and Bernstein[18] have analyzed the ^{90}Zr(α, α') reaction at 31 MeV and have pointed out that the long-range $1/r^{l+1}$ dependence of the Coulomb form factor implies the need to consider large impact parammeters and correspondingly large angular momenta. Kumabe *et al*[19] have analyzed the ^{90,91,92}Zr(α, α') reaction at 34.4 MeV and obtained the same conclusion. Thus all the present DWBA calculations shown in Figs. 4~6 have been carried out for $L_{max}=50$ and $R_{max}=25$ fm.

Trial calculations for a complex form factor including Coulomb excitation effect were also made. Calculated differential cross sections are only a few percent larger than those for real form factor but the patterns of calculated curves are vary similar to those for the real form factor, so that additional complication was not included in the remainder of the calculations.

The deformation parameters β_l's were determined by normalizing the individual calculated cross sections to the corresponding experimental data. The assumed spin-parities and deformation parameters of the excited states together with corresponding spin-parities obtained by other workers[6,20~25] are listed in Tables II and III.

Table II Excited states of ^{60}Ni

Present work			J^π				
level (MeV)	β_l	J^π	(α, α') 34 MeV[a]	(p, $p'\gamma$) 12 MeV[b]	(t, p)* 12 MeV[c]	^{60}Cu* decay[d]	(p, $p'\gamma$) 12 MeV[e]
1.33	0.200	2^+	2^+		2^+	2^+	2^+
2.16					2^+	2^+	2^+
2.29					0^+	0^+	0^+
2.50					4^+	4^+	4^+
3.11	0.061	2^+	2^+, (4^+)		$2^+ + 4^+$	2^+	$4^+ + 2^+$
3.35	0.035	2^+	2^+		$2^+(3^+)$	2^+	2^+
3.70	0.042	4^+	4^+		$1^+, 2^+$	1^+	(4^+)
4.04	0.160	3^-	3^-		3^-		3^-
4.30		$2^+ + 4^+$	4^+		$2^+(+4^+)$	2^+	2^+
4.50	0.038	2^+	2^+		2^+	2^+	2^+
5.01	0.080	5^-	5^-		4^+		5^-
5.11	0.072	4^+	4^+				4^+
5.25	0.047	2^+			4^+		4^+
5.39	0.049	3^-			3^-		
5.60	0.062	3^-	3^-				$(0^+, 3^-)$
5.80	0.041	2^+	2^+				
5.98	0.035	5^-					
6.16	0.072	3^-	3^-	3^-	$1^-, 3^-$		
6.34	0.046	2^+					
6.53	0.038	3^-	3^-	3^-	3^-		

* include summaries of previous works

[a] Ref. 6. [b] Ref. 20. [c] Ref. 21. [d] Ref. 22. [e] Ref. 23.

Table III Excited states of ^{62}Ni

Present work			J^π			
Level (MeV)	β_l	J^π	$(p, p\gamma')$ 12 MeV[a]	(n, γ)[b]	(t, p)* 12 MeV[c]	(γ, γ') 7.6 MeV[d]
1.17	0.184	2^+		2^+	2^+	2^+
2.02				0^+	0^+	0^+
2.30				2^+	$2^+(4^+)$	
2.32				4^+	4^+	
3.03	0.022	2^+		2^+		
3.16	0.044	2^+		2^+	2^+	0, 1, 2
3.27	0.075	4^+		$1^+, 2^+$	4^+	0, 1, 2
3.50	0.030	2^+		2^+	2^+	0, 1, 2
3.75	0.156	3^-		3^-	3^-	
4.01				$1^+, 2^+$		0, 1, 2
4.15	0.064	5^-		$2^+, 3^+$		
4.43	0.023	3^-		$1^+, 2^+$		
4.65	0.054	3^-		2, 3	0^+	
4.79	0.042	2^+				
5.00				1, 2		
5.31	0.053	2^+			(3^-)	
5.64	0.090	3^-			3^-	
5.93	0.051	2^+				
6.53	0.058	3^-	3^-			

* include summaries of previous works
[a] Ref. 20. [b] Ref. 24. [c] Ref. 21. [d] Ref. 25.

IV. 3. Coupled-channel calculations

Normally, the DWBA theory is carried only to first order in the deformation and therefore cannot predict differential cross sections for two-step processes such as the excitation of the two-phonon states. The two-phonon and one-phonon cross sections can be compared to results obtained from coupled-channel calculations. Datails of the formalism of the coupled-channel calculation have been described by Tamura.[26] The present calculations have been made by using Tamura's code "JUPITOR 1"*.

A real coupling including Coulomb excitation effect was used. A search was made on parameters β_{02}, β_{2I}, β'_{0I} and β''_{0I} to find best fits to the experimental data. Here β_{02} and β_{2I}(I=0, 2 and 4) appear linearly in the coupling matrices and connect 0^+_0(0^+_0 denotes the ground state) and 2^+_1, and 2^+_1 and I^+ states, respectively. The parameters β'_{0I} and β''_{0I} appear quadratically and linearly, respectively, in the coupling matrices and both connect the 0^+_0 and I^+ states. The parameter β'_{0I} was chosen to be $(\beta_{02}\beta_{2I})^{1/2}$. Therefoe we still have two free parameters β_{2I} and β''_{0I}.

The present calculations were made referring to Tamura's (α, α') work[7] on ^{60}Ni. Here β'_{0I} was chosen under the condition that the ratio β'_{0I}/β_{02} is equal to that obtained

* The code has been rewritten for a FACOM 230-60, IBM 360/75, HITAC-5020E by M. Wakai, S. Igarasi, O. Mikoshiba and S. Yamaji.

by Tamura.[7] For the 4_1^+ and 2_2^+ states the β''_{0I} values obtained by Tamura[7] were used in the present calculations and gave a fairly good agreement with the experimental data for the 4_1^+ states. However, for the 0_1^+ states a little modification of β''_{0I} values was needed to get good fits.

In coupled-channel calculations[26,27] for the inelastic proton scattering, the optical-

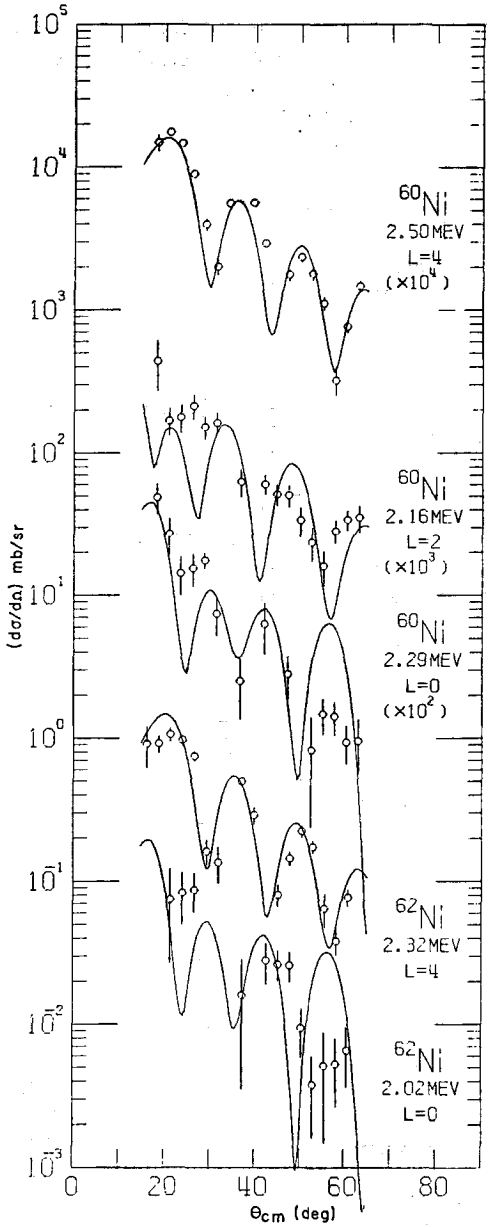

Fig. 7. Measured angular distributions for inelastic scattering leading to the so-called two-phonon states. The soild curves are the predictions of the coupled-channel theory.

Table IV The values of the parameter β used in the coupled-channel calculations

target	β_{02}	$r_0\beta_{02}$ (fm)	I	β_{2I}	β'_{0I}	β''_{0I}
^{60}Ni	0.200	0.316	0	0.110	0.148	−0.030
			2	0.155	0.176	+0.020
			4	0.190	0.195	+0.040
^{62}Ni	0.184	0.292	0	0.102	0.137	−0.020
			4	0.174	0.179	+0.040

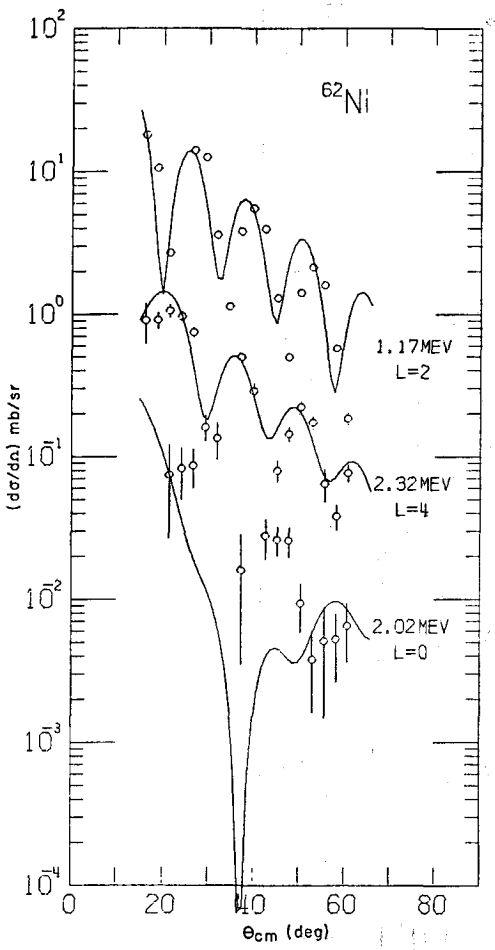

Fig. 8. Comparison of the measured angular distributions and the predictions of the DWBA calculation using the quasi-particle model form factors calculated by Glendenning and Veneroni.

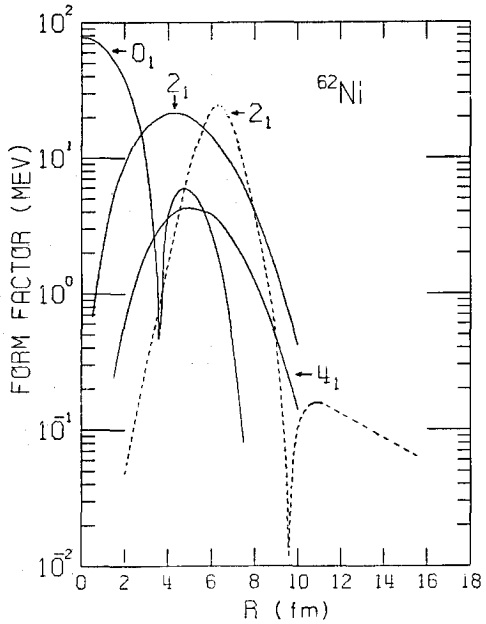

Fig. 9 Comparison of the form factors for the first 2^+, the first 4^+ and the first 0^+ states of ^{62}Ni. The scild curves are the quasi particle model form factors calculated by Glendenning and Veneroni. The dashed curve is the first derivative Saxon form factor. They are normalized to fit the present experimental cross sections.

model parameters were taken to be the same as those fixed in the fit to the elastic data with the exception of W for which different value was used to each channel. However for the inelastic alpha scattering the values of W used for the two-phonon channels are not known. Therefore we used $W=1.0\ W_{opt}$ for all channels. Calculated curves for the two-phonon states are shown in Fig. 7. The β-values used are listed in Table IV.

IV. 4. Microscopic analysis

Microscopic analyses for nickel isotopes have been developed by Glendenning and Veneroni[28] and by Madsen and Tobocman.[29] The angular distributions for the 2_1^+, 4_1^+ and 0_1^+ states of ^{62}Ni were analyzed here using form factors calculated from the microscopic model by Glendenning and Veneroni[28] and the INS-DWBA 2 code. In this microscopic description, the incident particle is assumed to act through a Gaussian force $V_o \exp(-\beta r^2)$ with the nucleons of the nucleus. The nuclear ground state is the BCS vacuum of quasi-particle pairs, and all the excited states are considered as two quasi-particle configuration mixings. The resultant form factors have been given in Ref. 28.

Figure 8 shows the calculated angular distributions and the experimental data. The form factors calculated from the microscopic model are compared with the derivative form factors of the macroscopic model in Fig. 9. The required depths of the potential of the Gaussian shape interaction V_o were 102, 126 and 147 MeV for the 2_1^+, 4_1^+ and 0_1^+ states, respectively.

V. DISCUSSION

V. 1. Elastic scattering

For alpha scattering, it is well known[16] that there are several sets of optical model parameters which give almost equally satisfactory fits to the experimental data.

A native picture of the alpha-nucleus interaction could envisage it as a simple superposition of four nucleon-nucleus optical potentials, suitably averaged over the internal motion of the alpha particle. Such a potential would have a real depth of order 200 MeV. A similar potential is obtained by averaging the known alpha-nucleon potential over the dansity distribution of the target nucleus. Experiments[30~32] in alpha-elastic scattering have been carried out at higher energies. These cross-section data have been analyzed by the respective authors in terms of the optical model, and results show that for data obtained at higher energies or extending over a large angular range, or both, the number or discrete sets of optical-potential parameters is smaller. For example, at 80 MeV for ^{24}Mg, with data limited to angles below 90°, Singh *et al.*[30] found four sets while with data up to 165° only one set was obtained. A potential determined uniquely in each higher energy work has a real depth of about 120 MeV.[30,31] Therefore the present automatic parameter search has also been carried out for $V=\sim 120$ MeV as is shown in Table I. As is seen in Table I, however, the present case shows a preference for the sets of potential parameters of depth V of about 50 MeV in all the cases.

For nickel isotopes, the set of potential parameters of depth V of about 200 MeV gave the best results for the 24 MeV data,[16] while the sets of about 50 MeV gave best

results for the 34 MeV data[6] and the 50 MeV data.[33]

Some of the authors and others[34] have investigated the elastic scattering of 109.2 MeV ^{3}He particles by ^{40}Ca, ^{58}Ni, ^{90}Zr and ^{116}Sn over a wide angular range, and they have found that the unique potential which fits the data has a real well depth of about 100 MeV.

V. 2. Spin-parity assignments

For the strongly excited levels at 1.33 and 4.04 MeV for ^{60}Ni and at 1.17 and 3.75 MeV for ^{62}Ni, the DWBA curves based on the one-phonon form factor produce excellent fits to the data. These levels are, of course, the well known 2^+ and 3^- collective levels. The fits to the remaining levels are not so definite. The fact that the high energy-resolution works have found many more levels in ^{60}Ni and ^{62}Ni in the energy range above 3 MeV indicates that the present peaks are groups of levels dominated by particulary strong ones. Such peaks dominated an assumed 2^+, 3^-, 4^+ or 5^- state are shown in Figs 4 and 5.

As is seen in Tables II and III for most of these levels spin-parity assignments are in good agreement with previous assignments. Angular distributions for the 4.01 and 5.00 MeV peaks of ^{62}Ni are peculiar and completely lack the usual oscillatory behaviour. Therefore, spin-parity assignments for these levels were impossible and the angular distributions are not shown in the figures.

In Fig. 6 the predicted angular distributions at large angles ($>65°$) are almost in phase with the experimental data, but their cross sections are not in such good agreement with the experimental data.

V. 3. The so-called two-phonon states

As is seen in Fig. 8, the general patterns of the angular distributions calculated from the microscopic model[28] for the 2_1^+ and 4_1^+ states are in agreement with the experimental data, but the angular distributions are shifted about two degrees toward smaller angles. On the other hand, the predicted angular distribution for the 0_1^+ state seems to be in phase with the experimental data, but shows an abnormal pattern.

As is seen in Fig. 7, the angular distributions obtained from the coupled-channel calculations for the 4^+ states of ^{60}Ni and ^{62}Ni are in fairly good agreement with the experimental data, although they are shifted about one degree toward smaller angles.

The predicted angular distribution for the 0_1^+ state of ^{60}Ni is in phase with the experimental data, while that of ^{62}Ni shows some indication of the shift in phase. And the overall slope of each predicted angular distribution shows a distinctly less sharp fall with angle.

The predicted angular distribution for the 2_2^+ state of ^{60}Ni is not in such good accordance with the experimental data.

It is concluded that the results of the present coupled-channel analyses for ^{60}Ni and ^{62}Ni at 28.5 MeV are similar with those[6] for ^{60}Ni at 34.4 MeV.

V. 4. Octupole states

Veje[9] has calculated excitation energies and reduced transition probabilities of 3^-

Table V Electromagnetic transition rates in single particle (Weisskopf) unit and EWSR fraction for inelastic scattering.

	Experiment			Theory	
	level (MeV)	G_3	S_3(%)	level (MeV)	G_3
^{60}Ni	4.04	18.6	13.0	4.07	26.1[a]
				4.08	26.7[b]
	5.39	1.7	1.6		
	5.60	2.8	2.7		
	6.16	3.8	4.0	6.25	4.0[a]
	6.53	1.1	1.2		
				7.30	0.20[a]
^{62}Ni	3.75	17.7	12.3	3.82	27.5[a]
	4.43	0.39	0.3		
	4.65	2.1	1.8		
	5.65	5.9	6.1		
	6.53	2.5	3.0	6.26	5.0[a]
				7.33	0.25[a]
^{58}Ni	4.45		13.7[c]		
	6.07		1.9[c]		
	(6.8 / 6.9)		5.8[c]		
	7.55		4.0[c]		
	7.9		2.7[c]		

[a] Ref. 9. [b] Ref. 8. [c] Ref. 6.

states, assuming a pairing plus octupole-octupole force which acts between particles. The $B(E3)$ values have been separated into two parts by cosidering isospin dependence and assuming that the inelastic alpha scattering gives rise $\Delta T=0$ excitation only.

Predicted excitation energies and predicted values of the electromagnetic transition rate G_3 in single particle (Weisskopf) unit are compared with the results of the present work in Table V. Following Bernstein,[18,35] the electromagnetic transition rate G_3 in single-particle (Weisskopf) unit was calculated from the β value obtained experimentally using the vibrations of a Fermi charge distribution. The ratios of the inferred electromagnetic transition rates for a Fermi charge distribution to those for a uniform charge distribution were taken from the table of Bernstein.[35]

The EWSR fraction S_l for a state with energy E_x is determined[36,10] from the deformation parameter β_l according to

$$S_l=\beta_l^2 E_x/\tilde{S}_l,$$

where for $l>0$ the sum rule limit $\tilde{S}_l$ is given for a uniform mass distribution by

$$\tilde{S}_l=l(2l+1)\frac{\hbar^2}{2mR^2}\frac{4\pi}{3A}.$$

Here A is the mass number, m is the nucleon mass and $R=1.2A^{1/3}$.

The EWSR fractions $S_3(\%)$ calculated are shown in Table V. The values of $S_3(\%)$ for ^{58}Ni were calculated from the 34 MeV (α, α') data[6] and are also shown in Table V. It may be concluded that for Ni isotopes several discrete octupole states between 4.5 and 8 MeV exhaust only $\sim$10% of the $E3$ strength allowed by EWSR.

ACKNOWLEDGMENTS

The authors wish to thank Professor T. Yanabu and the late Professor Y. Uemura for interests and encouragements throughout this work. They are also grateful to the cyclotron crew of the Instiute for Chemical Research, Kyoto University, for their kind operation of the cyclotron.

REFERENCES

(1) R.H. Bassel, G.R. Satchler, R.M. Drisko and E. Rost, *Phys. Rev.* **128**, 2693 (1962); E. Rost, *Phys. Rev.* **128**, 2708 (1962).
(2) B. Buck, *Phys. Rev.* **127**, 940 (1962); H.W. Broek, J.L. Yntema, B. Buck and G.R. Satchler, *Nucl. Phys.* **64**, 259 (1965).
(3) T. Tamura, *Nucl. Phys.* **73**, 81 (1965).
(4) See, for instance, I. Kumabe, H. Ogata, M. Inoue, Y. Ōkuma and J. Muto, *J. Phys. Soc. Japan* **19**, 147 (1964); R. Beurtey, P. Catillon, R. Chaminade, M. Crut, H. Faraggi, A. Papineau, J. Saudinos and J. Thirion, *Comp. Rend*, **252**, 1756 (1961); H.W. Broek, T.H. Braid, J.L. Yntema and B. Zeidman, *Proc. Rutherford Jubilee Int. Conf. Manchester, England* (1961) p. 517, G. Bruge, J.C. Faivre, H. Faraggi and A. Bussiere, *Nucl. Phys.* **A146**, 597 (1970), H. Rebel, R. Löken, G.W. Schweimer, G. Schatz and G. Hauser, *Z. Physik* **256**, 258 (1972).
(5) I. Kumabe, H. Ogata, S. Tomita, M. Inoue and Y. Ōkuma, *Phys. Lett.* **17**, 45 (1965).
(6) M. Inoue, *Nucl. Phys.* **A119**, 449 (1968).
(7) T. Tamura, *Progr, Theor, Phys. Suppl.* **37, 38**, 383 (1966).
(8) S. Yoshida, *Nucl. Phys.* **38**, 380 (1962).
(9) C.J. Veje, *Mat, Fys. Medd, Dan. Vid. Selsk.* **35**, No. 1 (1966).
(10) J.M. Moss, D.R. Brown, D.H. Youngblood, C.M. Rozsa and J.D. Bronson, *Phys. Rev.* **C18** 741 (1978).
(11) J.M. Moss, D.H. Youngblood, C.M. Rozsa, D.R. Brown and J.D. Bronson, *Phys. Rev. Lett.* **37**, 816 (1976); C. Mayer-Böricke, W. Oelert, A. Kiss, M. Rozsa, P. Turek and S. Wiktor, *Nucl. Phys.* **A293**, 189 (1977); T. Tohei, T. Hasegawa, K. Iwatani, M. Tanaka and S. Özkök, INS Annual Report (1977) p. 33.
(12) I. Kumabe, M. Matoba and E. Takasaki, *J. Phys. Soc. Japan* **25**, 301 (1968).
(13) S. Bashkin and G. Goldhaber, *Rev. Sci. Instrum.* **22**, 112 (1951).
(14) J.S. Blair, *Phys. Rev.* **115**, 928 (1959).
(15) M. Igarashi, "Automatic Search for Optical Potential Parameters" INS-PT-26 (1970).
(16) Lynne McFadden and G.R. Satchler, *Nucl. Phys.* **84**, 117 (1966).
(17) M. Kawai, K. Kubo and H. Yamaura, "INS-DWBA 2" INS-PT-9 (1965).
(18) E.J. Martens and A.M. Bernstein, *Nucl. Phys.* **A117**, 241 (1968).
(19) I. Kumabe, M. Matoba, H. Ogata, M. Inoue, Y. Ōkuma and T.H. Kim, *Bull. Inst. Chem. Res. Kyoto Univ.* **52**, 152 (1974).
(20) R. Ballini, N. Cindro, J. Delaunay, J. Fouan, M. Loret and J. *P.* Passerieux, *Phys. Lett.* **21**, 708 (1966).
(21) W. Darcey, R. Chapman and S. Hinds. *Nucl. Phys.* **A170**, 253 (1971).
(22) D.M. Van Patter and F. Rauch, *Nucl. Phys.* **A191**, 245 (1972).
(23) H. Ronsin, P. Beuzit, J. Delaunay, R. Ballini, I. Fodor and J.P. Fouan, *Nucl. Phys.* **A207**, 577 (1973).

(24) U. Fanger, D. Heck, W. Michaelis, H. Ottmar, H. Schmidt and R. Gaeta, *Nucl. Phys.* **A146**, 549 (1970).
(25) R. Moreh, A. Wolf, I. Jacob and A. Nof, *Nucl. Phys.* **A224**, 86 (1974).
(26) T. Tamura, *Rev. Mod. Phys.* **37**, 679 (1965).
(27) M. Sakai and T. Tamura, *Phys. Lett.* **10**, 323 (1964) ; P. L. Robinson, J. L. C. Ford, Jr., P. H. Stelson and G. R. Satchler, *Phys. Rev.* **146**, 816 (1966) ; P. H. Stelson, J. L. C. Ford, Jr., R. L. Robinson, C. Y. Wong and T. Tamura, *Nucl. Phys.* **A119**, 14 (1968) ; Y. Awaya, K. Matsuda, T. Wada, N. Nakanishi, S. Takeda and S. Yamaji, *J. Phys. Soc. Japan* **33**, 881 (1972).
(28) N. K. Glendenning and M. Veneroni, *Phys. Lett*, **14**, 228 (1965) ; *Phys. Rev.* **144**, 839 (1966).
(29) V. A. Madsen and W. Tobocman, *Phys. Rev.* **139**, B864 (1965).
(30) P. P. Singh, R. E. Malmin, M. High and D. W. Devins, *Phys. Rev. Lett.* **23**, 1124 (1969).
(31) B. Tatischeff and I. Brissaud, *Nucl. Phys.* **A155**, 89 (1970) ; H. Rebel, G. Hauser, G. W. Schweimer, G. Nowicki, W. Wiesner and D. Hartmann, *Nucl. Phys.* **A218**, 13 (1974).
(32) H. H. Duhm, *Nucl. Phys.* **A118**, 563 (1968) ; G. Hauser, R. Löhken, H. Rebel, G. Schatz, G. W. Schweimer and J. Specht, *Nucl. Phys.* **A128**, 81 (1969) ; P. P. Singh, W. T. Sloan, D. W. Devins and P. Shapiro, *Bull. Am. Phys. Soc.* **16**, 99 (1971) ; D. A. Goldberg, H. G. Pugh, P. G. Roos and S. M. Smith, *Bull. Am. Phys. Soc.* **16**, 1184 (1971) ; S. M. Smith and D. A. Goldberg, *Bull. Am. Phys. Soc.* **17**, 591 (1972).
(33) O. N. Jarvis, B. G. Harvey, D. L. Hendrie and J. Mahoney, *Nucl. Phys.* **A102**, 625 (1967).
(34) M. Hyakutake, M. Matoba, I. Kumabe, M. Fukada and T. Komatuzaki, *Nucl. Phys.* **A311**, 161 (1978).
(35) A. M. Bernstein, *Advances in Nuclear Physics* Vol. 3 p. 325 (1969).
(36) G. R. Satchler, *Nucl. Phys.* **A195**, 1 (1972).